CHAPTER 2 THEORY AND LITERATURE REVIEW

This chapter is divided into nine different sections. Detailed description of properties, processing and principle of electrolysis are presented in sections 2.1 - 2.3. Aspects of mass and ions transfer relevant to the calculation are described in section 2.4 and the concepts of mathematical modeling are introduced in section 2.5 and 2.6. In section 2.7, the pulse signal for the improvement of electrolysis system is described. The statistical analyses for experimental are presented in section 2.8 in which a detailed description of the relationship between variables and the factors affecting the hydrogen production rate and the efficiency are contained. Finally, in section 2.9, the literature review is accessed and incorporated at various stages in the research.

2.1 Hydrogen

Hydrogen is the lightest element and is a major factor in most of the organisms on Earth. It is estimated that 90% of the visible universe compose of hydrogen. Hydrogen combines with other elements to form numerous compounds. A large amount of hydrogen is combined with nitrogen from air to produce ammonia (NH_3) through a process called Haber process. Hydrogen is also added to fats and oils, such as peanut oil, through a process called hydrogenation. Liquid hydrogen is used in the study of superconductors and combined with liquid oxygen. Common chemical compounds are also provided for many elements. Some of the common ones are: water (H_2O), ammonia (NH_3), methane (CH_4), table sugar ($C_{12}H_{22}O_{11}$), hydrogen peroxide (H_2O_2) and hydrochloric acid (HCl). Based upon the oxidation number, an electronic configuration is also given. The term hydride is used in a generic sense to indicate compounds of the type M_xH_y and not necessarily to indicate that any compounds listed behave chemically as hydrides. In compounds of hydrogen, the most common oxidation numbers of hydrogen is 1.

Hydrogen has three isotopes, as shown in figure 2.1. By means of the mass spectrograph he had invented, Francis William Aston in 1927 observed that the line for hydrogen corresponded to an atomic weight on the chemical scale of 1.008. Other workers showed that the discrepancy could be removed by postulating the existence of a hydrogen isotope of mass 2 in the proportion of one atom of ^{2}H (D) to 4,500 atoms of ^{1}H. In 1931, Harold Urey detected deuterium by its atomic spectrum in the residue of a distillation of liquid hydrogen. Deuterium was first prepared in pure form by the electrolytic method of concentration. Tritium was discovered by physicists Ernest Rutherford, M. L. Oliphant, and Paul Harteck, in 1934. Each isotope has a different number of protons and number of neutrons (Aleinov and Schmidt, 2005; Schmidt, 2005; Schmidt et al., 2005) as follows:

- Protium (Hydrogen) has 1 proton with the atomic weight of 1.008 amu.
- Deuterium has 1 proton and 1 neutron with the atomic weight of 2.014 amu.
- Tritium has 1 proton and 2 neutrons with the atomic weight of 3.016 amu.

Deuterium and Tritium can occur naturally on earth, but in lower concentration while protium can occur under certain conditions. The normal state of hydrogen is molecular hydrogen (H_2) which is in low concentration of about 0.1 ppm in Earth's atmosphere. Hydrogen molecule has two forms: ortho-hydrogen and para-hydrogen. It is based upon on the rotation of the nucleus of an atom.

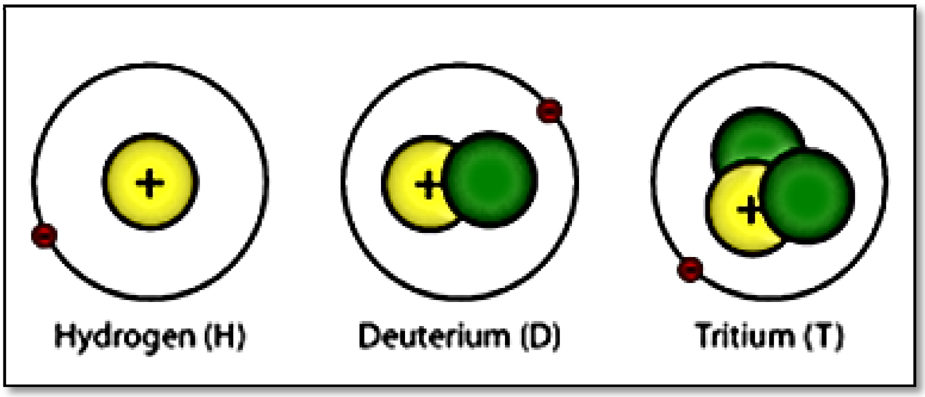

Figure 2.1 The three isotopes of hydrogen, showing their protons (marked in yellow, with positive charge), neutrons (green, with no charge), and electrons (red, with negative charge) (Schmidt, 2005)

2.1.1 Properties of Hydrogen

A phase diagram of hydrogen is shown in figure 2.2. At normal conditions hydrogen is in gaseous state. At atmospheric pressure, hydrogen is liquefied at -253°C, having the second lowest boiling point among all elements after helium, and solidified at -259°C. The boiling point of hydrogen is increased with the application of pressure, up to its critical point of -240°C at 13 atm (College of the Desert, 2001).

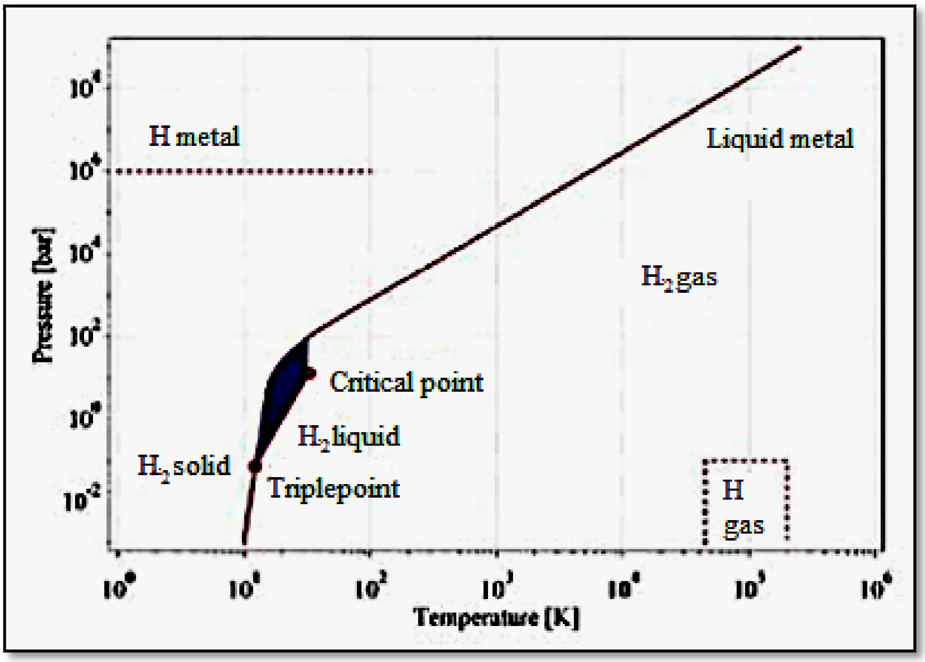

Figure 2.2 Simple phase diagram for hydrogen (Zuttel, 2003)

The physical properties of hydrogen are summarized in table 2.1. Ordinary hydrogen has a density of 0.09 kg/m^3. Hence, it is the lightest substance known with buoyancy in air of 1.2 kg/m^3. Solid metallic hydrogen has a greater electrical conductivity than any other solid elements. Also, the gaseous hydrogen has one of the highest heat capacity (14.4 kJ/kg K). Hydrogen has a low solubility in solvents; for example, at ambient conditions, only 0.018 and 0.078 mL of gaseous H_2 dissolves into each milliliter of water and ethanol, respectively (Gupta, 2009).

Table 2.1 Properties of hydrogen (Gupta, 2009)

Property	**Value**
Molecular weight	2.01594
Density of gas at 0°C and 1 atm.	0.08987 kg/m^3
Density of solid at −259°C	858 kg/m3
Density of liquid at −253°C	708 kg/m3
Melting temperature	−259°C
Boiling temperature at 1 atm.	−253°C
Critical temperature	−240°C
Critical pressure	12.8 atm.
Critical density	31.2 kg/m^3
Heat of fusion at −259°C	58 kJ/kg
Heat of vaporization at −253°C	447 kJ/kg
Thermal conductivity at 25°C	0.019 kJ/(ms°C)
Viscosity at 25°C	0.00892 centipoise
Heat capacity (C_p) of gas at 25°C	14.3 kJ/(kg°C)
Heat capacity (C_p) of liquid at −256°C	8.1 kJ/(kg°C)
Heat capacity (C^p) of solid at −259.8°C	2.63 kJ/(kg°C)

Hydrogen has three states (U.S. Department of Energy, 2001; Department of Alternative Energy Development and Efficiency Ministry of Energy) which are:

- Solid state, hydrogen is a colorless and is structured into six-sided crystals.
- Liquid state, hydrogen is a colorless. It has a lower viscosity and surface tension.
- Gas state, hydrogen is a colorless, odorless and non-toxic. At 273 K and 100 kPa, hydrogen gas has a mass of 0.0898 g. The important properties of hydrogen are presented in table 2.2.

Table 2.2 Thermal physical properties at various temperatures of hydrogen molecules in the gas state (Department of Alternative Energy Development and Efficiency Ministry of Energy)

T (K)	ρ (kg/m^3)	C_p (kJ/kg K)	$\mu \times 10^7$ (Ns/m^2)	$\nu \times 10^6$ (m^2/s)	$k \times 10^3$ (W/m K)	Pr
100	0.24255	11.23	42.1	17.4	67.0	0.707
150	0.16156	12.60	56.0	34.7	101	0.699
200	0.12115	13.54	68.1	56.2	131	0.704
250	0.09693	14.06	78.9	81.4	157	0.707
300	0.08078	14.31	89.6	111	183	0.701
350	0.06924	14.43	98.8	143	204	0.700
400	0.06059	14.48	108.2	179	226	0.6595
450	0.05386	14.50	117.2	218	247	0.689
500	0.04848	14.52	126.4	261	266	0.691
550	0.04407	14.53	134.3	305	285	0.685
600	0.04040	14.55	142.4	352	305	0.678
700	0.03463	14.61	157.8	456	342	0.675
800	0.03030	14.70	172.4	569	378	0.670
900	0.02694	14.83	186.5	692	412	0.671
1000	0.02424	14.99	201.3	830	448	0.673
1100	0.02204	15.17	213.0	966	488	0.662
1200	0.02020	15.37	226.2	1120	528	0.659
1300	0.01865	15.59	238.5	1279	568	0.655
1400	0.01732	15.81	250.7	1447	610	0.650
1500	0.01616	16.02	262.7	1626	655	0.643
1600	0.0152	16.28	273.7	1801	697	0.639
1700	0.0143	16.58	284.9	1992	742	0.637
1800	0.0135	16.96	296.1	2193	786	0.639
1900	0.0128	17.49	307.2	2400	835	0.643
2000	0.0121	18.25	318.2	2630	878	0.661

2.1.2 Heating Value

The heat capacity is the heat energy from the burning fuel. Higher value represents the total heat of the fuel. While the lower is removed by the latent heat energy, which is used in the condensation of water. The heat capacity of hydrogen compared to various fuels is presented in table 2.3. Table 2.3 concluded that the hydrogen has the highest heat capacity.

Table 2.3 The heat capacity of the fuel types (Department of Alternative Energy Development and Efficiency)

Fuel types	Lower Heating Value (MJ/kg)	Higher Heating Value (MJ/kg)
Hydrogen (g)	120.21	142.18
Natural gas (g)	47.141	52.225
Propane (l)	46.296	50.235
Butane (l)	45.277	49.210
Gasoline (l)	43.448	46.536
Methanol (l)	20.094	22.884

2.2 Hydrogen Production Processing

Hydrogen is produced from various sources, especially from hydrocarbons and water which are caused by the decay energy into electricity energy, thermal energy or chemical energy, etc (Rieger, 1994). Since the energy required for the production of hydrogen from hydrocarbons is lower than the electrolysis of the water, methods that are based on the use of hydrocarbons is widely used today. Therefore, most industrial hydrogen is produced from natural gas, oil and coal in which the hydrogen production process can be divided into three major guidelines below.

2.2.1 Thermal Process

Steam reforming: the principle of process is to supply steam into the system to react with hydrocarbons. During the process, hydrogen will be pulled from the hydrocarbon and water to become hydrogen gas. While the rest of carbon and oxygen is emerged as carbon monoxide gas. This process requires a solid catalyst to help in reducing the power consumption of the reaction. Usually the steam reforming is always associated with the water gas shift reaction especially when high amounts of vapor is fed into the system (Grimes et al., 2008; Zeng and Zhang, 2010).

Carbon dioxide reforming: this process is similar to steam reforming but the main difference is the use of carbon dioxide as a reactant by replacing steam. The advantage of this process is the use of carbon dioxide gas, which is toxic to the environment as a raw material in the hydrogen production. The disadvantage of the process is that the catalyst is deteriorated easily. The ratio of hydrogen production from this process is less than the steam reforming (Grimes et al., 2008; Zeng and Zhang, 2010).

Partial oxidation: PO_x is the thermal process between hydrocarbons and oxygen in the ratio that is not high enough to complete the combustion. The advantage is no external power source required due to partial oxidation process is exothermic. However, the limitation of the process is that the amount of oxygen entering into the system must not be too high because the rest of oxygen can react with hydrogen to produce water (Grimes et al., 2008; Zeng and Zhang, 2010).

Pyrolysis and gasification, this process is to heat the solid material such as biomass or coal under pressure in the reactor. In general, the pyrolysis and gasification are often occurred. Pyrolysis and gasification are the process of disintegration of the solid material into a gas because of heat sterilization of the system (Hulteberg and Karlsson, 2009).

2.2.2 Electrochemical Process

Electrochemical process is the production of high purity hydrogen (Kilic et al., 2008; Marangio et al., 2008; Oldham and Myland, 1994; Rieger, 1994) which is made through the electricity into the electrolyte solution. Production of hydrogen in this method does not cause dangerous gases or greenhouse effect. However, the hydrogen production by this way requires high energy to the reaction. Therefore, this production method is more expensive than others. (Grimes et al., 2008; Zeng and Zhang, 2010).

2.2.3 Photolytic Process

This method is biological process by bacteria and algae in the reaction. Groups of bacteria and algae have been of interest, such as Anaerobic bacteria, photo synthetic bacteria, cyan-bacteria and green algae, etc (Grimes et al., 2008). In principle, hydrogen gas is occurred by two main processes of the bio-photolysis and fermentation with the enzyme. Nowadays, efficiency of bio-hydrogen is still low but the advantage of this process is the low power consumption which leads to lower-price investment (Conibeer and Richards, 2007; Zeng and Zhang, 2010).

2.3 Principle of Electrolysis

For the past couple of hundred years we have come to rely more and more on fossil fuels, such as natural gas and coal. They also have the disadvantage of producing a variety of pollutant and greenhouse gases (CO_2, CO, NO_x) which in the discovery sheds light on climate change research, are problematic in that the processes require subsequent filtering and carbon sequestration technologies. Electrolysis is one method by which hydrogen can be produced cleanly from renewable sources as water. The splitting of water using electrolysis especially when coupled with renewable energy sources has fewer air pollution impacts than do fossil-fuel sources of hydrogen. Electrolysis requires electricity to power the process in which the source of this electricity determines the cleanliness of the process and the hydrogen fuel (Saur, 2008). Many different types of electrolysis cells have been proposed and constructed. The different electrolysis cell can be divided into groups based on the electrolyte. Table 2.4 presents an overview of the different types of cells which are capable of using H_2O as a reactant to produce H_2. However, only the solid oxide cell is also capable of using CO_2 to produce CO (Jensen et al., 2008).

Table 2.4 Electrolysis cells and their specialties (Jensen et al., 2008)

Type	Alkaline	Acid	Polymer electrolyte	Solid oxide
Charge carrier	OH^-	H^+	H^+	O^{2-}
Reactant	Water	Water	Water	Water, CO_2
Electrolyte	Sodium, Potassium hydroxide	Sulphuric, Phosphoric acid	Polymer	Ceramic
Electrodes	Nickel	Graphite with Pt, Polymer	Graphite with Pt, Polymer	Nickel, Ceramics
Temperature	80°C	150°C	80°C	850°C

The overall electrolysis reaction ($H_2O \rightarrow H_2 + ½O_2$ or $CO_2 \rightarrow CO + ½O_2$) is a sum of two electrochemical reactions (also called half-cell reactions), which occur at the electrodes. The electrode where the reduction of reactants or intermediates takes place is called the cathode. The anode is the electrode where oxidation of reactants or intermediates takes place. Both H_2O and CO_2 electrolysis become increasingly heat consuming with temperature. Hence at elevated temperatures a significant part of the total energy demand can be provided as heat according to figure 2.3. This provides an opportunity to utilize the Joule heat that is inevitably produced due to the passage of electrical current through the cell (Jensen et al., 2008).

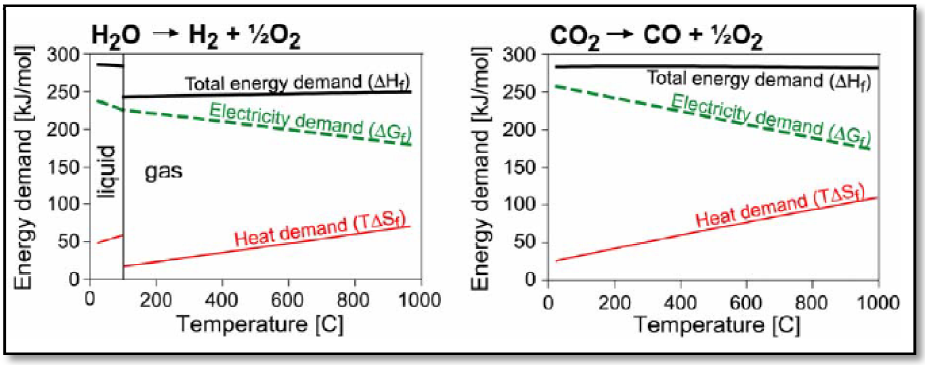

Figure 2.3 Thermodynamics of H_2O and CO_2 electrolysis at 0.1 MPa (Jensen et al., 2008)

An alkaline water electrolyzer has been developed in this work due to its low cost and uncomplicated technology. The alkaline water electrolyzer consists of electrodes (anode and cathode), an electrolyte solution, a power supply and a container (Grimes et al., 2008; Oldham and Myland, 1994; Rieger, 1994). Figure 2.4 shows the schematic diagram of the electrolyte solution. Direct current is applied to electrodes, leading to a flow of electrons from the power supply. The electrochemical reactions for alkaline water electrolysis are shown in Eqs.R1 and R2.

At anode: $2OH^- \rightarrow 1/2O_2 + H_2O + 2e^-$ R1
At cathode: $2H_2O + 2e^- \rightarrow H_2 + 2OH^-$ R2
Net: $H_2O \rightarrow H_2 + 1/2O_2$ R3
$\Delta H = -288\ \mathrm{kJmol^{-1}}$

The direct current maintains the electron flow from the negative terminal of the direct current source to the positive terminal at which the electrons are consumed by water to form hydrogen gas and hydroxyl ions. The hydroxyl ions transfer through the electrolyte solution to the anode, at which the hydroxyl ions give away electrons and these electrons return to the positive terminal of the direct current source, producing oxygen gas (Grimes et al., 2008). Therefore, hydrogen is produced at the cathode and oxygen is produced at the anode and the overall reaction of the alkaline water electrolysis is shown in Eq.R3 (Oldham and Myland, 1994; Rieger, 1994) where water is decomposed into hydrogen and oxygen gases.

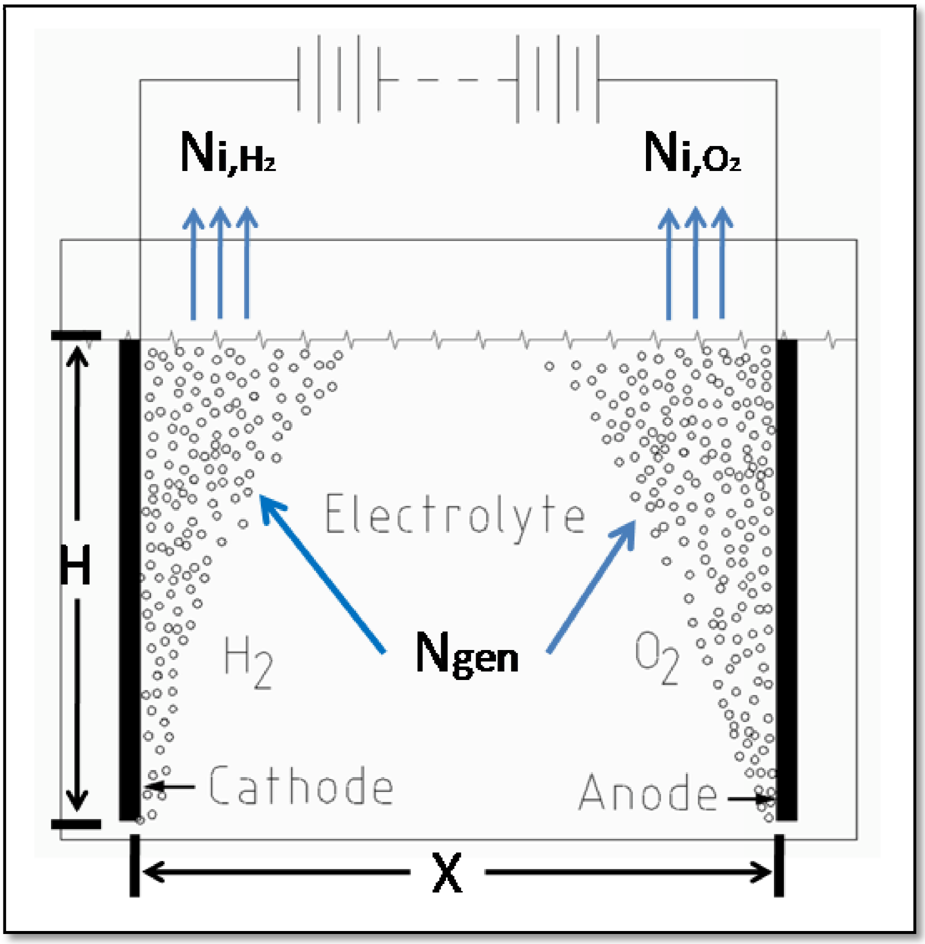

Figure 2.4 The schematic diagram of the electrolyte solution

It is well known that electrolysis process is an irreversible reaction which requires external energy input into the system. Initially, the current flowing through the electrolyte is gradually increased in small increments until the voltage is greater than 1.23 voltages, so the gas bubbles flow up from the two electrodes. The current can be increased rapidly by adding a potential as shown in figure 2.5. If the straight line is drawn from the curve to meet the electrode potential axis (at $I = 0$) the intercept on the potential axis is decomposition potential which is the minimum potential required for continuous electrolysis and is the same as the reversible potential.

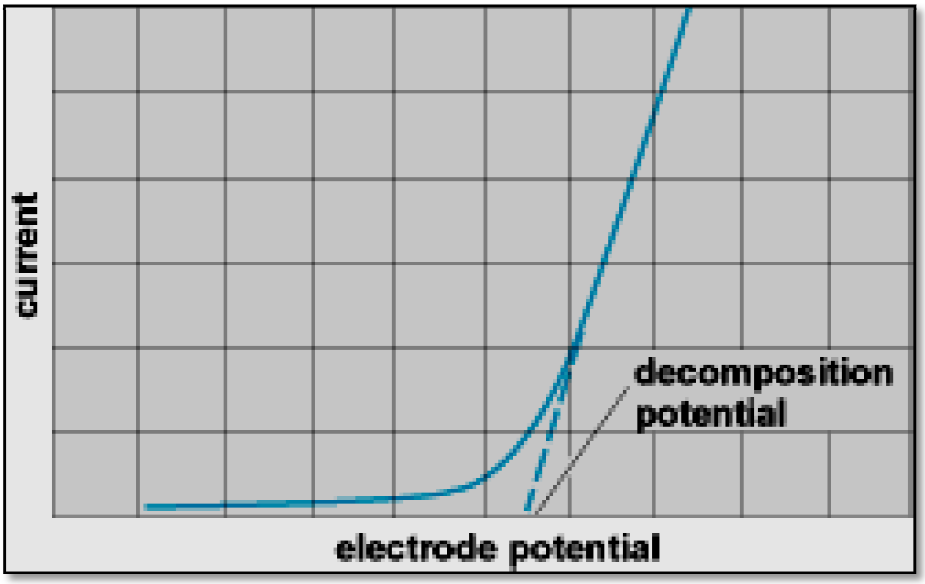

Figure 2.5 The relationship between current and electrode potential in the electrolysis cell (AccessScience, 2013)

Polarization can be classified into three categories according to the characteristics including the concentration polarization, the activation polarization and the ohmic polarization which is caused by discontinuities in the transfer of electrons to the electrode surface. The minimum polarization required for any electrode can occur at an appreciable rate under given condition. Polarization makes the reaction difficult in that it requires the energy to process. However energy losses, associated with reaction kinetics as well as charge transport through electrical leads and the electrolyte, necessitate electrolyzer operation in this voltage regime. In the case of practical devices the operating voltage can be expressed as Eq. 2.1 (Grimes, 2008; SØrensen, 2004).

$$E_{op} = E_{rev} + E_{ohm} + E_{con} + E_{act} \tag{2.1}$$

where, E_{op} is electrolysis cell potential, E_{rev} is reversible potential, E_{ohm} is ohmic potential, E_{con} is concentration potential and E_{act} is activation potential.

2.3.1 Reversible Potential

At standard ambient temperature and pressure, the change in Gibb's free energy (ΔG) for the water splitting reaction in Eq.R3 is positive and hence the reaction is non-spontaneous. In an electrolysis cell the electrical energy is supplied by applying a potential difference between two electrodes placed in an electrolyte. Electrical energy to chemical energy conversion takes place at the electrode-solution interface through charge transfer reactions. A potential difference, E, applied between the electrodes can be used to do maximum work (E_0) of nFE, where F is the Faraday constant and n is the number of moles of electrons involved in the reaction. E_{rev} ,is the minimum voltage needed to drive the water splitting reaction as shown in Eq. 2.2 (Grimes, 2008).

$$\Delta G = nFE_{rev} \tag{2.2}$$

The reaction at this voltage is endothermic and hence at isothermal conditions heat energy (TΔS, where S is entropy and T is the absolute temperature) must be absorbed from the surrounding environment for the increase in entropy associated with water dissociation. On operating an electrolysis cell above E_{rev}, heat is generated due to the losses in the cell and a fraction of this provides the additional energy needed for the entropy change. When energy exactly equal to the enthalpy $\Delta H = \Delta G + T\Delta S$ (=285.83 kJ/mol at 1 bar and 25°C) for water splitting is supplied, no heat is absorbed or evolved by the system (Grimes,2008; JANAF, 1971).

2.3.2 Ohmic Potential

Current flow between electrodes in electrochemical cells is occurred through the electrolyte phase and current is described in terms of a solution resistance for the electrolyte between the electrodes. The magnitude of this resistance depends on the ionic conductivity of the electrolyte, as described above, and also on the geometric arrangement of electrodes in the cell (Zoski, 2007). Reduction in the electrode separation and electrolyte-resistance lowers the Ohmic overvoltage (Casper, 1978; Divisek and Wendt, 1990; Nagai et al., 2003). Bubble formation by the product gases is also a source of activation and Ohmic overpotentials (de Jonge et al., 1982; Nagai et al., 2003; Roy et al., 2006; Sillen et al., 1982). An increase in operating temperature helps to reduce both activation and Ohmic overvoltages as it enhances the reaction rate and reduces the electrolyte resistance. Overvoltage minimization is the electrolysis cells as shown in Eq. 2.3.

$$E_{ohm} = IR_{cell} \tag{2.3}$$

The resistance for microdisk electrode and planar electrodes can be found in Eqs. 2.4 and 2.5, respectively.

$$R = \frac{1}{(4r)(k)} \tag{2.4}$$

$$R = \frac{L}{(A)(k)} \tag{2.5}$$

where, L is the distance between planar electrodes, A is the area of electrode, k is the electrolyte conductivity and r is the disk radius of microdisk electrode.

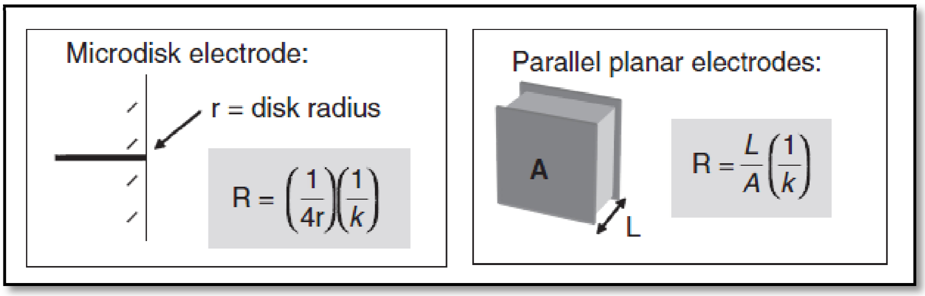

Figure 2.6 Relationship between solution resistance and cell geometry for two limiting cases of electrodes in contact with electrolytes (Zoski, 2007)

The dependence of solution resistance on cell and electrode geometry is complicated for the general case and requires integration over the full three dimensional geometry of the cell for a rigorous solution. Figure 2.6 presents two such cases: one for a disk electrode embedded in an insulator and immersed in an electrolyte phase, and the other for a pair of parallel planar electrodes with an electrolyte phase interposed between them. The figure includes equations for estimating the solution resistance using only the electrolyte conductivity and parameters relating to electrode size and spacing for the calculation.

2.3.3 Concentration Potential

Although the work of Faraday had established early on the relationship between the current generated during electrolysis and the amount of generated species, the dependence of cell potential on the concentration of electroactive species remained theoretically elusive until the advent of thermodynamics. By considering the following reduction reaction in Eq. R4 (Zoski, 2007).

$$O+ne^{-}\rightleftarrows R \tag{R4}$$

where, O is the oxidized species, R is the reduced species, and n is the number of electrons exchanged between O and R, the relationship between the concentration of oxidized species $[O]$, concentration of reduced species $[R]$, and free energy (ΔG) is given as shown in Eq.2.6 (Bard and Faulkner, 2001; Zoski, 2007).

$$\Delta G=\Delta G^{0}+RT\ln\frac{[R]}{[O]} \tag{2.6}$$

where, R is the universal gas constant. The mathematical expression describing the correlation between potential and concentration for a cell reaction is a central tenant of electrochemistry and is known as the Nernst equation obtained by combining Eqs. 2.2 and 2.6 as shown in Eq.2.7 (Bard and Faulkner, 2001; Rieger,1994; Zoski, 2007).

$$E=E^{0}+\frac{RT}{nF}\ln\frac{[R]}{[O]} \tag{2.7}$$

2.3.4 Activation Potential

The potential of an electrode strongly affects the kinetics of reactions occurring on its surface. Hydrogen evolves rapidly at some potential, but not at the others. So potentials is for all faradaic processes because the interfacial potential difference can be used to control reactivity. In developing a theory of electrode kinetics, it is convenient to express potential against a point of significance to the chemistry of the system, rather than against an arbitrary external reference. There are two natural reference points: the equilibrium potential of the system and the standard (or formal) potential of the couple under consideration. From Eq.R4, species O and R engage in a one-electron transfer at the interface without being involved in any other chemical step. Suppose also that the standard free energy profiles along the reaction coordinate have the shapes shown in figure 2.7. The upper frame of that figure depicts the full path from reactants to products, while the lower frame is an enlargement of the region near the transition state (Bard and Faulkner, 2001).

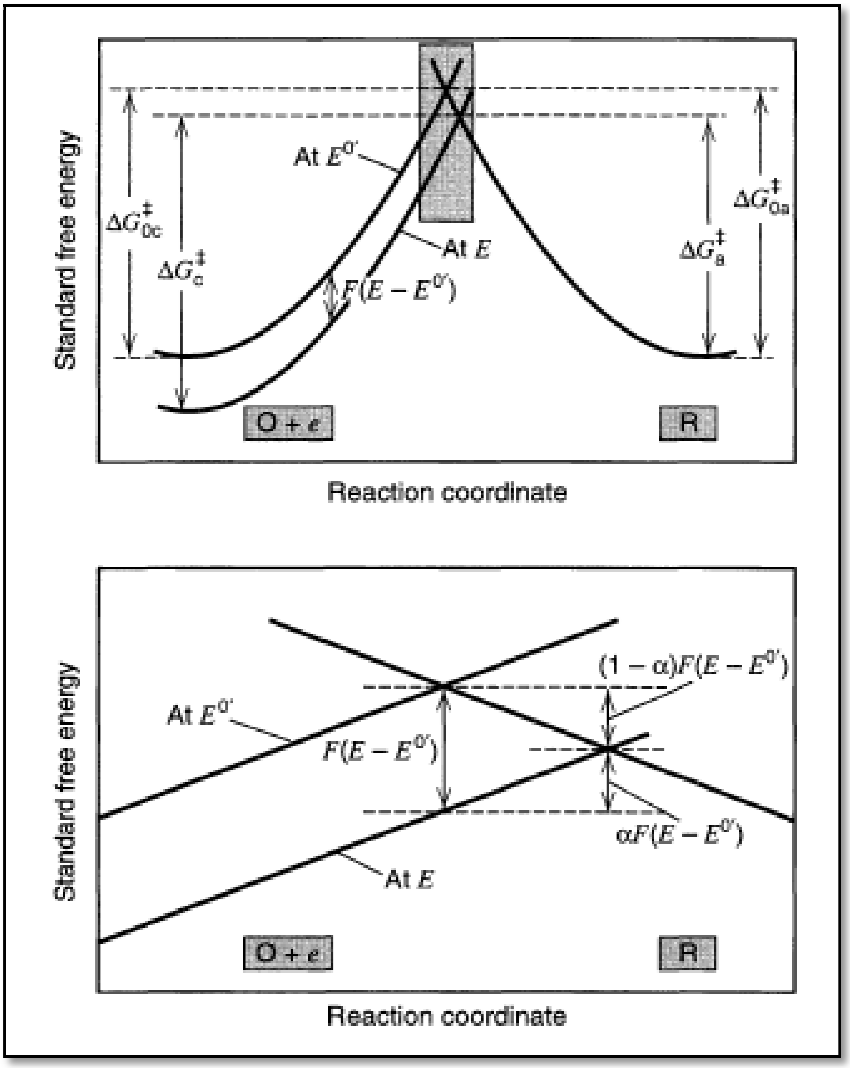

Figure 2.7 Effect of a potential change on the standard free energies of activation for oxidation and reduction (Bard and Faulkner, 2001) Note: The lower frame is a magnified picture of the boxed area in the upper frame

Chemical kinetics of the transfer reactor can be described by the Butler Volmer's equation which is used for calculating activation potential. This activation potential is based on current density and temperature as shown in Eq. 2.8.

$$i = i^0 \left[\exp\left(\frac{\alpha_{an} F E_{act}}{RT_{an}}\right) - \exp\left(\frac{\alpha_{cat} F E_{act}}{RT_{cat}}\right) \right] \tag{2.8}$$

From Eq. 2.8, E_{act} at the anode and cathode can be expressed as shown in Eqs 2.9 and 2.10.

$$E_{act,an} = \frac{RT_{an}}{\alpha_{an} F} \ln \frac{i}{i_{0,an}} \tag{2.9}$$

$$E_{act,cat} = \frac{RT_{cat}}{\alpha_{cat} F} \ln \frac{i}{i_{0,cat}} \tag{2.10}$$

where, T_{an} is the temperature on the anode, T_{cat} is the temperature on the cathode, $i_{0,an}$ is the current density on the anode (A/cm^2), $i_{0,cat}$ is the current density on the cathode (A/cm^2), i is the current density (A/cm^2) and α_{an} and α_{cat} is the coefficient for the one-electron reaction of the anode and the cathode, respectively.

2.4 Modes of Mass and Ions Transfer in Electrolytes

Mass transfer, that is, the movement of material from one location in solution to another, arises either from differences in electrical or chemical potential at the two locations or from movement of a volume element of solution. Mass transfer can be accomplished in three different ways and/or a combination of these modes.

1. Diffusion

Movement of a species under the influence of a gradient of chemical potential (i.e., a concentration gradient).

2. Migration

Movement of a charged body under the influence of an electric field (a gradient of electrical potential).

3. Convection

Generally fluid flow occurs because of natural convection (convection caused by density gradients) and forced convection such as stirring or hydrodynamic transport, and may be characterized by stagnant regions, laminar flow, and turbulent flow.

Most of these are expressed as equations of concentration dynamics, that is, concentration of one or more solution species as a function of time, as well as other variables, in the form of differential equations as shown in Eq.2.11. Fundamentally, these are transport equations but may be complicated by chemical processes occurring heterogeneously or homogeneously. The transport components are all included in the general Nernst-Planck equation (Bard and Faulkner, 2001; Britz, 2005).

$$J_j = -D_j \nabla C_j - \frac{z_j F}{RT} D_j C_j \nabla \phi + C_j v \qquad (2.11)$$

where J_j is the molar flux per unit area of species j at the given point in space, D_j is the diffusion coefficient of species, C_j is the concentration gradient, z_j is charge, v is the rate with which a volume element moves in solution, ϕ is the potential gradient and ∇ denotes the differentiation operator and it is directional in 3-D space. In Eq.2.11, the first term is concerned with the diffusion and is, in fact, Fick's first law, the second term accounts for the migration of the species in the solution, and the last term represents the convection of the solution.

2.4.1 Faraday's Law

The number of reactant molecules involved in an electrode reaction is related stoichiometrically to the number of charges (electrons) flowing in the circuit. This is the basic argument of the laws formulated by Michael Faraday in 1832–1833. Faraday's first law reads: In electrolysis, the quantities of substances involved in the chemical change are proportional to the quantity of electricity which passes through the electrolyte. Faraday's second law reads: The masses of different substances set free or dissolved by a given amount of electricity are proportional to their chemical equivalents. Faraday's law correlates the total charge, Q, passed through a cell to the amount of product, N, as expressed in Eq. 2.12 (Bagotsky, 2006 ; Zoski, 2007).

$$Q=nFN \tag{2.12}$$

where F is Faraday's constant, $F = 96{,}485.3\ \mathrm{C\ mol^{-1}}$, and n is the number of electrons transferred per mole of product. Faraday's law can be used in many applications, such as electrogravimetry and coulometry which to find the total amount of electricity required for complete electrolysis of a compound. It can also be used for finding the number of electrons implicated in an electrolysis process (Zoski, 2007).

2.4.2 Rate of Reaction

In order to grasp what is taking place in an electrochemical reaction, the concept of current and how the current changes when a stimulus is applied must be understood. The current is equal to the change in charge with time.

$$i = \frac{dQ}{dt} \tag{2.13}$$

where i [A] is the faradaic current, t [sec] is the time, and Q [C] is the charge given by Faraday's law. Chemical reactions can be either homogeneous or heterogeneous. The first type occurs in a single phase, and its rate is uniform everywhere in the volume as shown in Eq. 2.14 (Bard and Faulkner, 2001; Zoski, 2007).

$$Rate[mol \bullet \sec^{-1}] = \frac{dN}{dt} \tag{2.14}$$

Heterogeneous reactions occur at the electrode-solution interface, and they are characteristic of electrochemistry. While the expression for the reaction rate is similar to Eq.2.14 it depends upon the area of the electrode, A [cm^2], or the area of the phase boundary where the reaction occurs as shown in Eq. 2.15 (Zoski, 2007).

$$Rate[mol \bullet \sec^{-1}] = \frac{i}{nFA} \tag{2.15}$$

2.4.3 Fick's Laws of Diffusion

Fick proposed two laws of diffusion in solution. These equations describe the relation between the flux of a substance and its concentration as a function of both time and position. The first law describes the flux of a species, O, as a function of the change in its concentration, C_O, with distance, *x*, from an electrode, at a time *t* as shown in Eq.2.16 (Zoski, 2007).

$$J_0(x,t) = -D_0 \frac{\partial C_j(x,t)}{\partial x} \tag{2.16}$$

From the point of view of an experimentalist that has to interpret data, it is desirable to reduce the complexity of the equations that govern the mass transfer. Alternatively, the solution can be stirred so fast that the flux *J* becomes a function of convection only. The flux can also be written as found in Eq.2.17.

$$J = \frac{1}{A}\frac{dN}{dt} \tag{2.17}$$

Eqs.2.12 - 2.17 can be combined to get the expression for the mass transfer limiting current as shown in Eq. 2.18.

$$i = nFAmC \tag{2.18}$$

2.4.4 Electrical Double Layer

The solution side of the double layer is thought to be made up of several "layers." That closest to the electrode, the inner layer, contains solvent molecules and sometimes other species (ions or molecules) that are said to be specifically adsorbed as shown in figure 2.8. This inner layer is also called the compact, Helmholtz, or Stern layer. The locus of the electrical centers of the specifically adsorbed ions is called the Inner Helmholtz Plane (IHP), which is at a distance x_1. The total charge density from specifically adsorbed ions in this inner layer is $\sigma^1(\mu C/cm^2)$. Solvated ions can approach the metal only to a distance x_2; the locus of centers of these nearest solvated ions is called the Outer Helmholtz Plane (OHP). The interaction of the solvated ions with the charged metal involves only long-range electrostatic forces, so that their interaction is essentially independent of the chemical properties of the ions. These ions are said to be nonspecifically adsorbed. Because of thermal agitation in the solution, the nonspecifically adsorbed ions are distributed in a three-dimensional region called the diffuse layer, which extends from the OHP into the bulk of the solution. The thickness of the diffuse layer depends on the total ionic concentration in the solution; for concentrations greater than 10^{-2} M, the thickness is less than $\sim 100\overset{\circ}{A}$. The potential profile across the double-layer region is shown in figure 2.9. The variable ϕ, is called the inner potential (Bard and Faulkner, 2001).

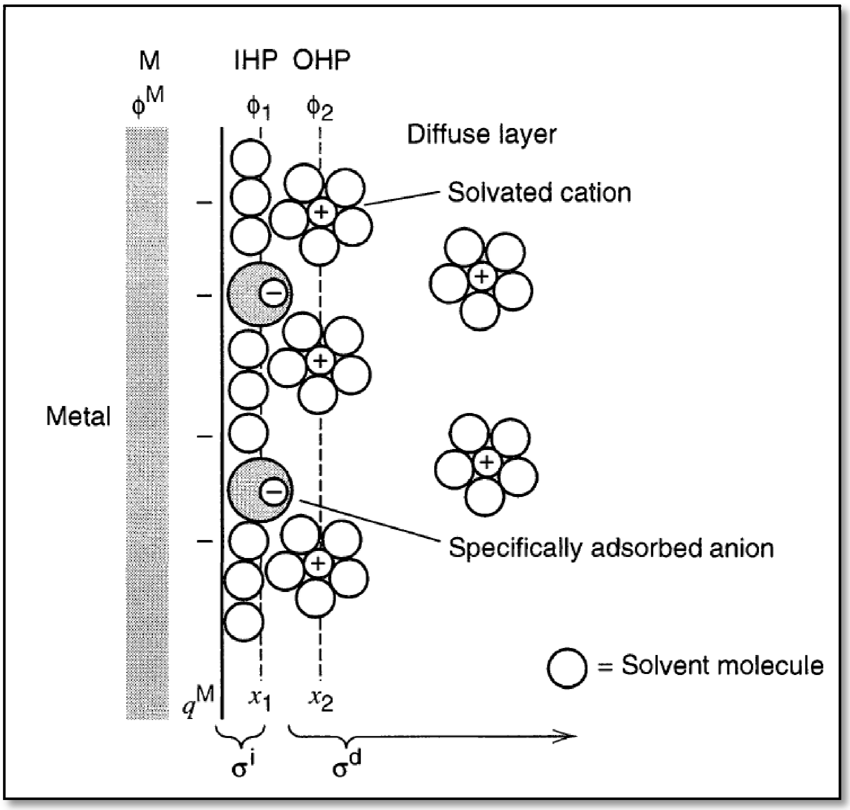

Figure 2.8 Proposed model of the double-layer region under conditions where anions are specifically adsorbed (Bard and Faulkner, 2001)

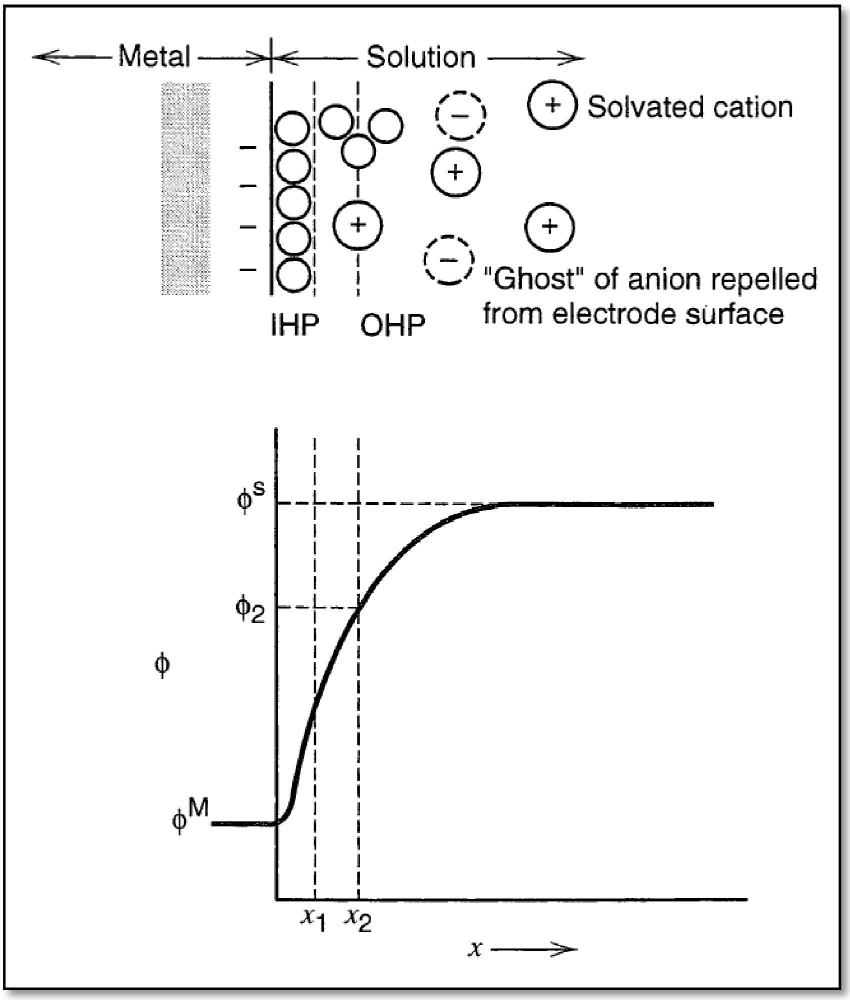

Figure 2.9 Potential profiles across the double-layer region in the absence of specific adsorption of ions (Bard and Faulkner, 2001)

2.5 Electrolyte Conductivity

One of the most important qualities that a medium must process to be useful in electrochemical science is an ability to support current flow. Electrochemical reactions always produce or consume ions at electrodes, and the electrolyte provides the pathway for ions to flow between and among electrodes in the cell to maintain charge balance. The ability of a phase to support current flow by motion of charged particles (ions in an electrolyte) when an electric field exists within the phase is called the conductivity, usually abbreviated as σ_B. It has unit of ohm^{-1} cm^{-1}, sometimes called Siemens cm^{-1}. Conductivity is a property of a phase or material, for an electrolyte phase of uniform cross section of area *A* and length *L*, whose electrical resistance is *R* where the ionic conductivity is given by $\sigma_B = \frac{1}{R}\frac{L}{A}$. Ionic conductivity in electrolytes depends on two main factors: (i) the concentration of free charge carriers (ions) and (ii) the ability of the charge carriers (ions) to move in an electric field (Zoski, 2007). The mixture conductivity (σ_B) is determined from the void fraction. It is decreased due to the presence of the gas in the electrolyte and can be calculated using Bruggeman correction as articulated in Eq. 2.19.

$$\sigma_B = \sigma_0 (1 - \alpha_{total})^{1.5} \tag{2.19}$$

where σ_0 is the conductivity with no bubbles and α_{total} is the total void fraction. In addition to the transport of charge, the current flow in an electrolyte is also accompanied by mass transfer. The species mass flux in dilute solution can be calculated using Planck-Nernst law. The conductance of the solution which is the reciprocal of the resistance, is given by Ohm's law. Under electroneutrality state and no current, I = 0 is set and σ_0 can be written as uttered in Eq.2.20.

$$\sigma_0 = \frac{F^2 |Z_i|^2}{R'T} (C_{i+} D_{i+} + C_{i-} D_{i-}) \tag{2.20}$$

2.6 Model of Void Fraction

The void fraction is one of the most important parameters used to characterize two phase flows. It is the key physical value for determining numerous other important parameters, such as the two-phase density and two phase viscosity, for obtaining the relative average velocity of the two phases. The void is of fundamental importance in models for predicting flow pattern transitions, heat transfer and pressure drop. Various geometric definitions are used for specifying the void fraction: local, chordal, cross-sectional and volumetric, which are represented schematically in figure 2.10. The local void fraction (α_{local}) refers to that at a local point and thus α_{local} = 0 when liquid is present and α_{local} = 1 when vapor is present. Typically, the local time-averaged void fraction is cited, or measured using probe, which represents the fraction of time vapor, was present at that location in the two phase flow. If $P_k(r,t)$ represents the local instantaneous presence of vapor or not at some radius "r" from the channel center at time t, then $P_k(r,t)$ = 1 when vapor is present and $P_k(r,t)$ = 0 when liquid is present. Thus, the local time-averaged void fraction is defined as expressed in Eq.2.21 (Thome, 2010).

$$\alpha_{local}(r,t) = \frac{1}{t}\int_t P_k(r,t)dt \tag{2.21}$$

The chordal void fraction ($\alpha_{chordal}$) is typically measured by shining a narrow radioactive beam through a channel with a two phase flow inside, calibrating its different absorptions by the vapor and liquid phases, and then measuring the intensity of the beam on the opposite side, from which the fractional length of the path through the channel occupied by the vapor phase can be determined. The chordal void fraction is defined as articulated in Eq.2.22 (Thome, 2010).

$$\alpha_{chordal} = \frac{L_G}{L_G + L_L} \tag{2.22}$$

where L_G is the length of the line through the vapor phase and L_L is the length of the line through the liquid phase.

The cross-sectional void fraction (α_{c-s}) is typically measured using either an optical means or by an indirect approach. The cross-sectional void fraction is defined as seen in Eq.2.23 (Thome, 2010).

$$\alpha_{c-s} = \frac{A_G}{A_G + A_L} \tag{2.23}$$

where A_G is the area of the cross-section of the channel occupied by the vapor phase and A_L is that of the liquid phase.

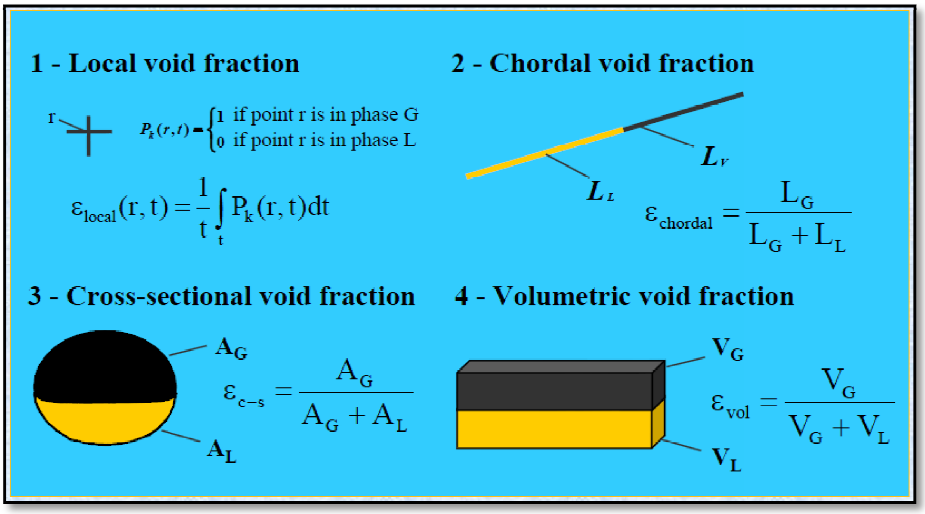

Figure 2.10 Geometrical definitions of void fraction: local, chordal, cross-sectional and volumetric (Thome, 2010)

The volumetric void fraction (α_{vol}) is typically measured using a pair of quick-closing values installed along a channel to trap the two phase fluid, whose respective vapor and liquid volumes are then determined. The volumetric void fraction can be defined by Eq.2.24 (Thome, 2010).

$$\alpha_{vol} = \frac{V_G}{V_G + V_L} \tag{2.24}$$

where V_G is the volume of the channel occupied by the vapor phase and V_L is that of the liquid phase.

2.7 Pulse Signal

The parameters needed to define a pulsating electrolysis process are time-on and time-off periods that can be used to calculate duty cycle, frequency and average current density as shown in figure 2.11 and Eqs. 2.25-2.27.

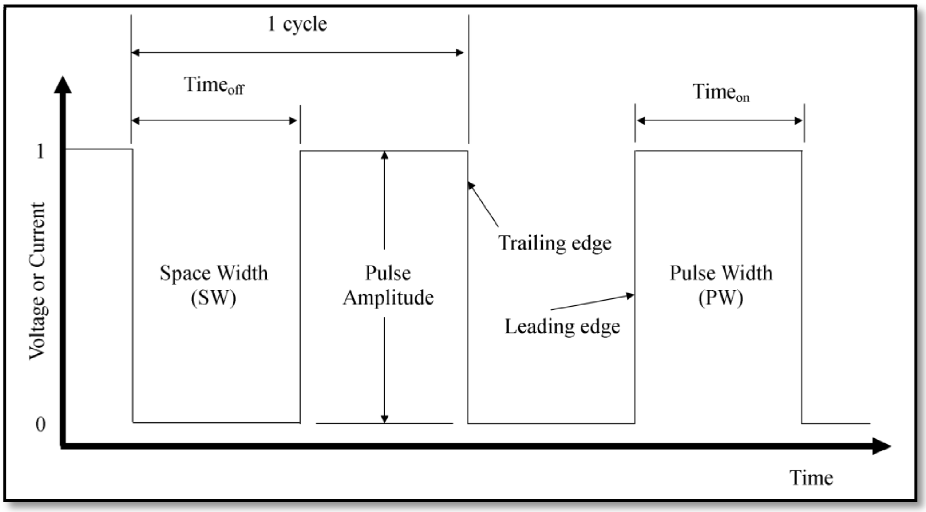

Figure 2.11 Components of the pulse signal

$$DutyCycle = \frac{time_{on}}{time_{on} + time_{off}} \times 100\% \tag{2.25}$$

$$Frequency = \frac{1}{time_{cycle}} = \frac{1}{time_{on} + time_{off}} \tag{2.26}$$

$$Average\ Current\ Density = I_p \times DutyCycle \tag{2.27}$$

where, $time_{on}$ is time-on periods, $time_{off}$ is time-off periods, $time_{cycle}$ is time of 1 cycle, I_p is peak current, t_d is time interval between negative edge of voltage and current signal and t_r is time interval between positive edge of voltage and current signal.

2.8 Statistical Analysis

In selecting the response variables, it should be certain that the variables really provide useful information about the process under study. Most often, the average or standard deviation of the measured characteristic will be the response variable. Multiple responses are not unusual. Gauge capability is also an important factor. If gauge capability is inadequate, only relatively large factor effects will be detected by the experiment or perhaps additional replication will be required. In some situations where gauge capability is poor, each experiment unit may be measured several times and use the average of the repeated measurements. It is usually important to identify issues related to defining the responses of variable and how they are measured before conducting the experiment. Sometimes designed experiments are employed to study and improve the performance of measurement systems.

2.8.1 Procedure of Decision Analysis

This section describes factor analysis, particularly suitable for analyzing the patterns of complex, multidimensional relationships encountered. It defines and explains in broad, conceptual terms of the fundamental aspects of factor analytic. Factor analysis can be utilized to examine the underlying patterns or relationships for a large number of variables and to determine whether the information can be condensed or summarized in a smaller set of factors or components. To further clarify the methodological concepts, guidelines for presenting and interpreting the results are also included (Hair et al., 2006).

The factor analysis can be divided into seven stages. Figure 2.12 shows the first three stages of the structured approach to multivariate model building, and figure 2.13 describes the final three stages, plus an additional stage (stage 7) beyond the estimation, interpretation, and validation of the factor models, which aids in selecting surrogate variables, computing factor scores, or creating summated scales for use in other. The procedure of each state is shown as follows.

Stage 1: Objectives of factors analysis

The starting point in factor analysis, as with other statistical techniques, is the research problem. In meeting its objectives, factor analysis is keyed to four issues: specifying the unit of analysis, achieving data summarization and/or data reduction, variable selection, and using factor analysis results.

Stage 2: Designing a factor analysis

The design of a factor analysis involves three basic decisions: (1) calculation of the input data (a correlation matrix) to meet the specified objectives of grouping variables or respondents; (2) design of the study in terms of number of variables, measurement properties of variables, and the types of allowable variables; and (3) the sample size necessary, both in absolute terms and as a function of the number of variables in the analysis.

Stage 3: Assumptions in factor analysis

The critical assumptions underlying factor analysis are more conceptual than statistical. In factor analysis the overriding concerns center as much on the character and composition of the variables included in the analysis as on their statistical qualities. A strong conceptual foundation needs to support the assumption that a structure does exist before the factor analysis is performed. A statistically significant Bartlett's test (significant < 0.05) indicates that sufficient correlations exist among the variables to proceed. Measure of Sampling Adequacy (MSA) values must exceed 0.50 for both the overall test and each individual variable; variables with values less than 0.50 should be omitted from the factor analysis one at a time, with the smallest one being omitted each time.

Stage 4: Deriving factors and assessing overall fit

Once the variables are specified and the correlation matrix is prepared. Decisions must be made concerning (1) the method of extracting the factors (common factor analysis versus components analysis) and (2) the number of factors selected to represent the underlying structure in the data.

Stage 5: Interpreting the factors

Although no unequivocal processes or guidelines determine the interpretation of factors to assist in the process of interpreting a factor structure and selecting a final factor solution, three fundamental processes are described. Within each process, several substantive issues (factor rotation, factor-loading significance, and factor interpretation) are encountered. Thus, after each process is briefly described, each of these processes will be discussed in more details. An optimal structure exists when all variables have high loadings only on a single factor. Variables that cross-load (load highly on two or more factors) are usually deleted unless theoretically justified or the objective is strictly data reduction. Variables should generally have communalities of greater than 0.50 to be retained in the analysis. Respecification of a factor analysis can include such options as follows: Deleting a variable, Changing rotation methods and Increasing or decreasing the number of factors.

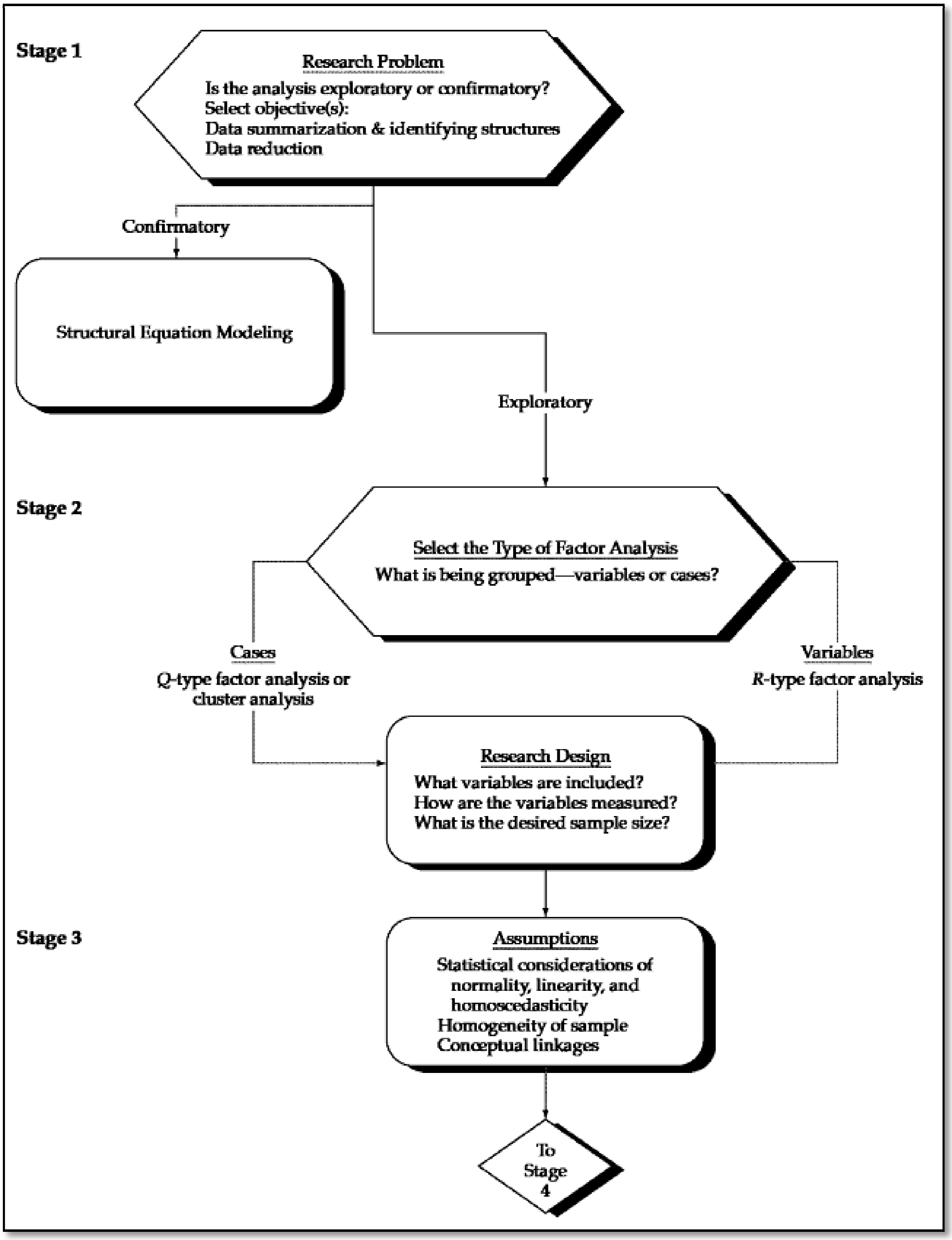

Figure 2.12 Stages 1-3 in the factor analysis decision diagram (Hair et al., 2006)

Stage 6: Validation of factor analysis

The sixth stage involves assessing the degree of generalizability of the results to the population and the potential influence of individual cases or respondents on the overall results. The issue of generalizability is critical for each of the multivariate methods, but it is especially relevant for the interdependence methods because they describe a data structure that should also be representative of the population.

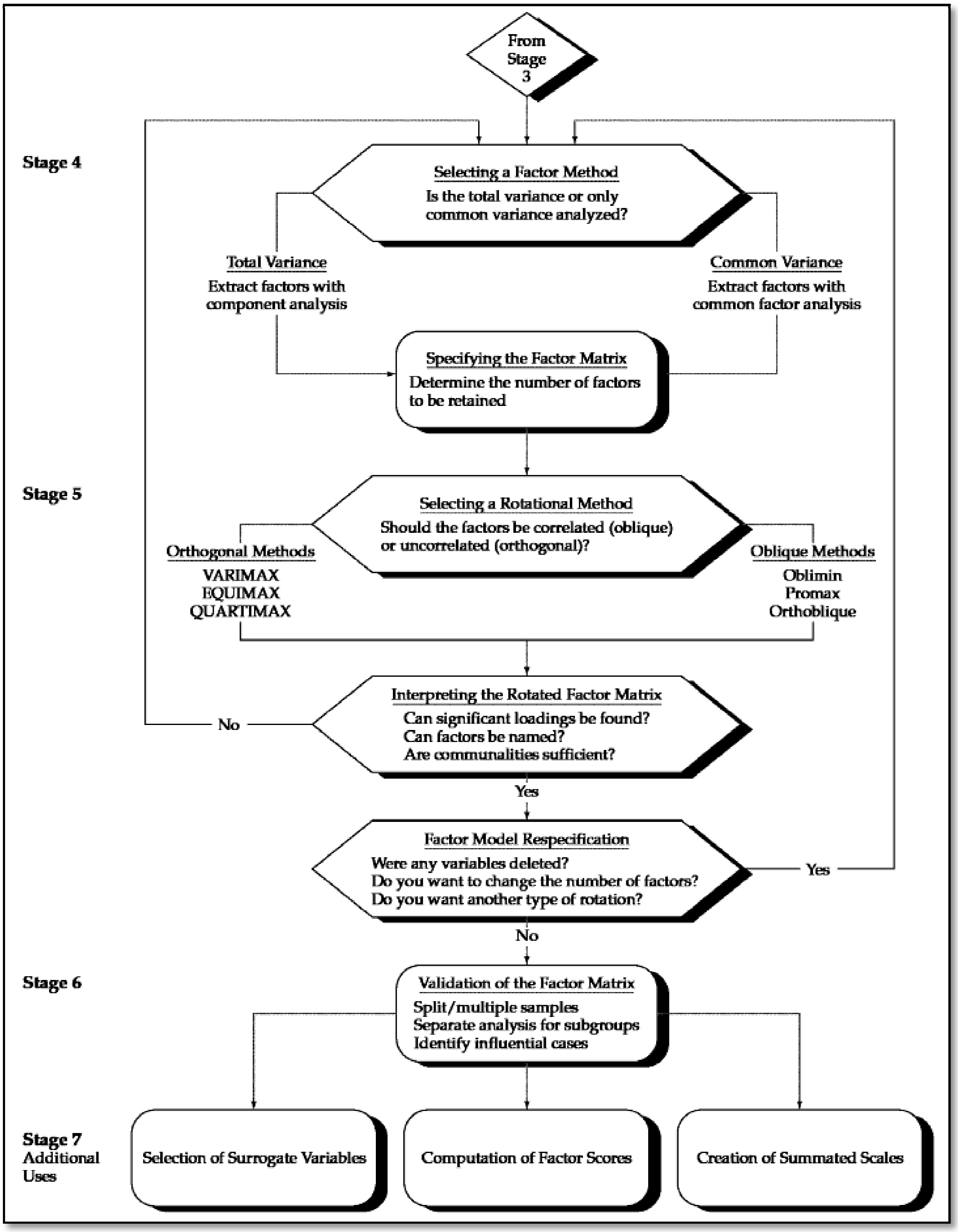

Figure 2.13 Stages 4-7 in the factor analysis decision diagram (Hair et al., 2006)

Stage 7: Additional uses of factor analysis results

Depending upon the objectives for applying factor analysis, the researcher may stop with factor interpretation or further engage in one of the methods for data reduction. If the objective is simply to identify logical combinations of variables and better understand the interrelationships among variables, then factor interpretation will suffice. It provides an empirical basis for judging the structure of the variables and the impact of this structure when interpreting the results from other multivariate techniques. If the objective, however, is to identify appropriate variables for subsequent application to other statistical techniques, then some form of data reduction will be employed. The two options include the following: Selecting the variable with the highest factor loading as a surrogate representative for a particular factor dimension and replacing the original set of variables with an entirely new, smaller set of variables created either from summated scales or factor scores.

2.8.2 The Fitting Regression Model

The response Y is dependent on k, for X_1, X_2... X_p as shown in figure 2.14. The relationship between these variables is characterized by a mathematical model called a regression model which presents the results of an experiment. The fitting regression model develops an empirical model relating the amount of current and the electrolyte temperature. Regression model is a collection of mathematical and statistical techniques that are useful for the modeling and analysis of a problem in which a response of interest is influenced by several variables and a response of interest is then optimized. The form of the relationship between the response (Y) and the factors (x_i) is given by Eq. 2.28, which is called the second-order model. It is used for a polynomial of higher degree (Hair et al., 2006 and Montgomery, 2001).

$$Y=\beta_0+\sum_{i=1}^{k}\beta_i x_i+\sum_{i=1}^{k}\beta_{ii}x_i^2+\sum\sum_{i<j}\beta_{ij}x_i x_j+\varepsilon \tag{2.28}$$

where β_0 is the arithmetic mean value of the responses, β_i corresponds to the factor effects, β_{ii} is the quadratic effects and β_{ij} is the interactions between the various factors. The ε variable stands for the fitting error. Almost all RSM problems use one or both of these models. It is likely that a polynomial model will be a reasonable approximation of the true functional relationship over the entire space of the independent variables.

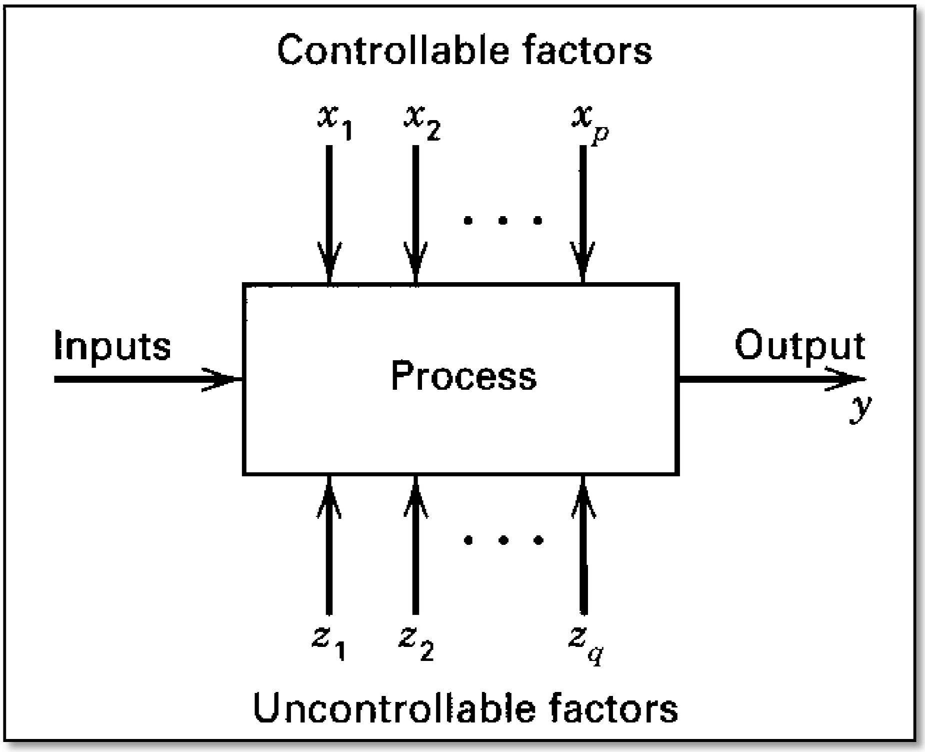

Figure 2.14 General model of a process or system (Montgomery, 2001)

Statistical methods should be used to analyze the data so that results and conclusions are objective rather than judgmental in nature. If the experiment has been designed correctly and if it has been performed according to the design, the statistical methods required are not elaborate. There are many excellent software packages designed to assist in data analysis and many of the programs used in procedure to select the design provide a seamless, direct interface to the statistical analysis. Often it finds that simple graphical methods play an important role in data analysis and interpretation. Because many of the questions can be cast into a hypothesis-testing framework, hypothesis testing and confidence interval estimation procedures are very useful in analyzing data from designed experiment. It is also usually very helpful to present the results of many experiments in terms of an empirical model, which is an equation derived from the data that expresses the relationship between the response and the important design factors. Residual analysis and model adequacy checking are also important analysis techniques (Hair et al., 2006 and Montgomery, 2001). Once the data have been analyzed, practical conclusions about the results and recommend a course of action can be drawn. Graphic methods are often useful in this stage, particularly in presenting the results to others. Follow up runs and confirmation testing should also be performed to validate the conclusions from the experiment.

2.9 Literature Review

The theoretical and experimental research is studied in literature to investigate mass transfer of ions and flow mechanisms of bubble. Attention has drawn to a study of factors that affect the gas production and energy usage. It has been observed that several parameters have effects on the hydrogen production rate. Factors involved in this hydrogen production process include types of solution, pH, current density (Dieguez et al., 2008; Kilic et al., 2008; Ursua et al., 2009), distance between electrodes, types of electrode material (Zhigang et al., 1999), solution concentration (Boll et al., 2003), pressure, temperature (Biaku et al., 2008; Grigoriev et al., 2009; Roy et al., 2006; Santarelli et al., 2009), types of power supply (Dieguez et al., 2008; Ursua et al., 2009) and solution flow rate (Kilic et al., 2008; Marangio et al., 2009).

Ulleberg (2003) developed a mathematical model of alkaline electrolyzer. This model has evolved the theory of thermodynamic systems, heat transfer and chemical relationships of power that can be integrated into the solar cell system. Mathematical model described the energy equation of electrolyzer was preferred in terms of the heat capacity of the electrolyzer which was 174kJ°C^{-1} while the heat losses was approximately 4.3 W(m^{2}°C)$^{-1}$ and thermal resistance was 0.164 °CW^{-1}. Perron et al. (2007) developed a mathematical model calculating the total resistance in the form of Laplace equation and used Finite Element Method (FEM) to analyse the effect of morphology of the bubble layer (position, size and shape of each bubble) on the gas productivity. They found that the relative resistance (R_t/R_0) ratio of the total resistance (R_t) to the electrolyte resistance in the absence of bubbles (R_0) was increased with an increase of bubble diameter. Aldas and Mat (2005) and Aldas (2004) created mathematical model for the two-phase flow in an electrochemical cell. It was found that both current density and bubble size had an effect on the gas release rate which affected the velocity profile in the electrochemical cell. Caspersen et al. (2012) modeled electrolyte conductivity under natural convection and found that the model provided clear tendency for electrolyte conductivity from combinations of current density, pressure and electrolyte width.

Dieguez et al. (2008) worked on the thermal performance of the alkaline electrolyzer. In a study, two types of power supply (EPS and IGBT-based electronic converter (EC)) were used and it was found that the temperature of the electrolyzer was increased rapidly when the power supply EPS was used as a result of the circuit arrangement in the device. Ursua et al. (2009) studied the nature of electric power supply. It was found that by supplying a half phase, energy loss was occurred, higher than that of a full-bridge. The hydrogen production rate was proportional to the electricity supply. Boll et al., (2003) conducted a research on electrolyzer at high temperature and pressure. At high temperature, potential was decreased while the higher pressure resulted in higher potential power.

In addition, the void fraction also has an effect on buoyancy of the bubble formed during the reaction. Matsushima et al. (2006) studied the effect of the bubble under gravity and microgravity and reported that fine gas bubble formed a bubble layer in alkaline solution, whereas bubble frequently coalesced in acidic solution. Gas bubble movements were reflected in the coalescence number and bubble resistance time. Golnabi et al. (2009) studied the characteristic physical properties of electrical conductivities of pure, distilled, municipal, river and industrial water liquids. It was found that a change in physical properties of the solution would have an effect on the electrical conductivity. The gas bubbles in the electrolyte solution, in the terminal electrodes and within the electrolyzer can cause the change of the resistance of the electrolyte solution during the time of gas production. Van Damme et al. (2010) presented the algorithm of bubble nucleation for gas evolving electrodes including bubble growth driven and electrode surface blocking. Aldas et al. (2008) studied void fraction distribution and found that the local void fraction was slightly underestimated. Weijs et al. (1997) investigated the resistance of the solution and found that the gas voidage in the solution was a function of the distance of the gas-evolving electrode and the absence of gas bubbles in the bulk solution. Sarkar et al. (2010) studied and aimed at determining the hydrogen bubble size generated as a function of current density and electrode geometry. It was found that current density had no influence on the detachment diameter and the nucleation rate was increased with increasing current density. This is consistent with the work reported by Nagai et al. (2003) who studied the effect of bubble occurring between electrodes through the void fraction between electrodes. The results showed that an increase of void fraction between electrodes by decreasing the electrode space brought about to a decrease of the electrolysis efficiency.

Ohmic resistance is a type of electrical resistance, which can cause a voltage loss according to Ohm’s law. The electrolyzer resistance varies with wire and connector resistance, electrodes resistance (anode and cathode), bubble resistance (hydrogen and oxygen bubble) and electrolyte ions resistance. Hydrogen and oxygen gas bubble are formed on electrode surface. The gas bubble covering the electrode surface is assumed as an additional electrical resistance to the system. Therefore, the bubble phenomenon is relevant to parameters such as bubble rise, the space between electrodes and pressure (Nagai et al., 2003, Roy et al., 2006 and Santarelli et al., 2009). In the electrochemical system, moving charges between electrodes and the electrolyte are electrons and ions. In most electrolyzers, due to its larger size, ion charge transport is far more difficult than electron charge transport, thereby resulting in the resistance to charge transport as a voltage loss. Because this voltage loss obeys Ohm’s law, it is called an "ohmic", or "IR loss". Ohmic loss consists of resistance of electrodes (R_{elec}) and resistance of ionic (R_{ionic}) (electrolyte) (Marangio et al., 2009 and O’Hayre, 2009).

From previous relevant research, it can be seen that there are factors affecting the hydrogen production and the efficiency in the electrolysis process, such as temperature, pressure, concentration, current density, types of electrodes, flow rate of solution, etc. Therefore, in this research, some factors (the amount of current, temperature, current characteristic, materials, electrolyte solution, concentration and surface area) affecting the incidence of hydrogen production are studied and used as guidelines in developing electrolyzers. In addition, this research aims to study the effects of the alkaline electrolysis reaction in the form of electrolyte conductivity via both numerical and empirical models and to compare them with the experimental results. The numerical model gives a relation to the equations of the physical property, while the empirical model is presented with the aim of confirming the numerical results and the results will be subsequently discussed.